Research Square

Preprints are preliminary reports that have not undergone peer review.
They should not be considered conclusive, used to inform clinical practice,
or referenced by the media as validated information.

Evaluation of tortuosity based on an experimental study of a solute diffusion in a porous medium

Denis Polezhaev
Perm State Humanitarian-Pedagogical University
Anastasia Teryokhina
teryokhina_av@pspu.ru

Perm State Humanitarian-Pedagogical University

Research Article

Keywords: porous medium, porosity, tortuosity, diffusion coefficient

Posted Date: July 15th, 2026

DOI: https://doi.org/10.21203/rs.3.rs-10164053/v1

License: This work is licensed under a Creative Commons Attribution 4.0 International License.
Read Full License

Additional Declarations: No competing interests reported.

Version of Record: A version of this preprint was published at Transport in Porous Media on August 12th, 2026. See the published version at https://doi.org/10.1007/s11242-026-02346-w.

Evaluation of tortuosity based on an experimental study of a solute diffusion in a porous medium

D. A. Polezhaev and A. V. Teryokhina

Perm State Humanitarian Pedagogical University, Perm, 614000, Russia.

*Corresponding author(s). E-mail(s): teryokhina_av@pspu.ru;
Contributing authors: polezhaev@pspu.ru;

Abstract

This paper presents the experimental findings of measurements of the tortuosity of a porous medium obtained using a technique based on comparing the molecular diffusion coefficient of a solute in a free fluid with the diffusion coefficient of the same solute in the fluid filling the pores. Water is used as the solvent, with the fluorescent dye Rhodamine B acting as the solute. The porous medium is modeled using a thin rectangular cell filled with monosized hard spheres. The models differ in cell thickness and sphere diameter, allowing the porosity of the medium to be varied between 0.40 and 0.55. The porosity and the shape of the porous medium skeleton influence the tortuosity, which in the conditions of this study varies from 1.20 to 1.46. The obtained data on diffusion tortuosity are compared with theoretical predictions for porous media with a skeleton consisting of hard spheres, as well as with experimental findings by other authors.

Keywords: porous medium, porosity, tortuosity, diffusion coefficient

1 Article Highlights

- A new experimental technique for measuring diffusion tortuosity τ_d is proposed
- The relation $\tau_d - P$ is examined in a range of porosities $P > 0.4$ that had not previously been studied experimentally
- The new results are in good agreement with the known data in the limit of close packing of hard spheres

2 Introduction

Tortuosity is a key way of measuring the geometry and transport properties of porous materials such as sedimentary rocks, soils, and catalyst particles. In the literature, tortuosity has been defined as either a geometric parameter or one that is related to the hydraulic, electrical, or diffusive properties [1].

The present paper discusses a technique for calculating the diffusion tortuosity of a porous medium by measuring the diffusion coefficient of a solute in the fluid filling the pores of the porous medium. With obstacles in their way, solute molecules are forced to take a longer path in a porous material. Longer pathways result in smaller displacement and, consequently, an apparent diffusion coefficient D_p that is less than its corresponding free fluid value D_m. Then, the diffusion tortuosity τ_d can be defined as the ratio of the molecular diffusion coefficient of species in free fluid D_m to the diffusion coefficient of species in a porous medium D_p [2–4]. It can therefore be concluded that the tortuosity of a porous medium is always greater than unity.

The practical importance of evaluating the tortuosity of porous materials and the complexity of this problem have attracted the attention of many researchers over the decades. This resulted in the development of diverse models that establish correlations between tortuosity (of geometric, electrical, hydraulic, or diffusive nature) and other properties of porous media. Notably, laws relating tortuosity to porosity have become widely accepted (porosity P is the relative fraction by volume of the fluid contained within a porous material). Among others, we may note relations in which the tortuosity is linearly dependent on porosity [5], varies according to a power-law [6–8], or a logarithmic law [9]. In all scenarios, the tortuosity decreases as porosity increases (the tortuosity must tend to one as $P \to 1$). For a more complete view of these relations, we refer the reader to the review papers [1, 4, 10].

It appears evident that the numerous relations between tortuosity and porosity will result in a variety of findings for a given porous medium. Even more pronounced differences are observed when considering porous media with distinct pore geometries. Therefore, there are a variety of semi-empirical relations available in the literature for calculating tortuosity as a function of porosity involving variables that depend on both the tortuosity nature and the pore morphology. In this respect, theoretical and experimental research can be classified into two broad categories. The first category comprises studies investigating tortuosity in soils, sediments, porous rocks, etc. [11–14]. The second category includes studies of porous media consisting of spheres [9, 15, 16], cubic and parallelepipedal particles [15, 17], cylinders [18, 19], and particles of other shapes [20, 21].

The objective of this study is to measure the diffusion tortuosity of a model porous medium consisting of a layer of identical hard spheres filling the space between wide parallel walls. To the best of our knowledge, there are very few theoretical and experimental studies investigating the relation $\tau_d - P$ in a wide range of porosity of a material whose skeleton consists of hard spheres. It is important to note that earlier experimental studies and the present research differ in terms of the techniques used to produce the samples of various porosities. In earlier studies, mixtures of hard spheres of varying diameters were utilized. The composition of the samples was modified, thus enabling the variation of porosity. In our experiments, we use identical hard spheres,

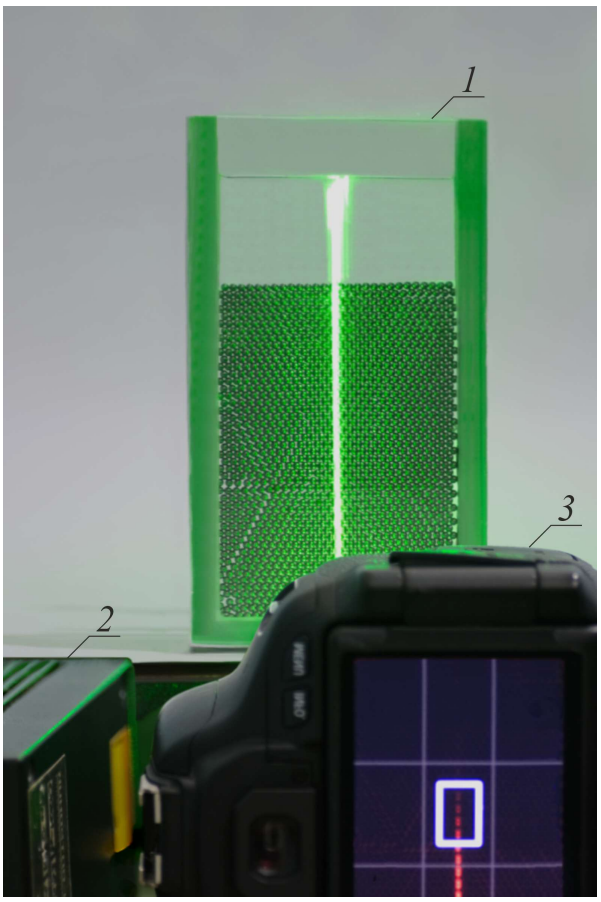


Figure 1 Photo of the experimental setup: A vertical rectangular cell filled with aqueous solution of Rhodamine B and hard spheres *1*, a laser that emits a green laser sheet *2*, a camera with orange filter *3*

but we vary the distance between the walls of the rectangular cell, which affects the total pore volume, i.e., the porosity.

3 Experimental Technique

The experiments are conducted in a rectangular cell (*1* in Fig. 1) of dimensions $l = 200$ mm in height and $b = 90$ mm in width, with thicknesses h that vary from 2.00 to 4.00 mm. The front and rear walls of the cell are made of 10-mm-thick transparent glass plates (Fig. 2). The gap thickness h between the glass plates is determined by the thickness of the U-shaped Plexiglas gasket, which is adhered to the glass plates.

The cell is filled with steel spheres with a diameter of $d_1 = 1.98 \pm 0.01$ mm, $d_2 = 3.00 \pm 0.01$ mm, or $d_3 = 3.98 \pm 0.01$ mm. In the experiments conducted with hard spheres of diameters d_2 and d_3, the cell thickness h is equal to the diameter of the spheres. In this configuration, the spheres within the cell are arranged in such a

Table 1 Parameters of porous media models

Number of a model	d, mm	h, mm	h/d	P	τ
M1	1.98 ± 0.01	2.00	1.01	0.40	1.45
M2	1.98 ± 0.01	2.19	1.11	0.44	1.37
M3	1.98 ± 0.01	2.48	1.25	0.50	1.28
M4	1.98 ± 0.01	2.70	1.36	0.55	1.20
M5	3.00 ± 0.01	3.00	1.00	0.43	1.46
M6	3.98 ± 0.01	4.00	1.00	0.41	1.43

manner that the centers of any three neighboring spheres from two different rows are positioned at the vertices of an equilateral triangle. This configuration of spheres is referred to as a hexagonal pattern, since each sphere has six neighbor spheres with which it is in contact. In addition to the contact between the neighboring spheres, each sphere also contacts both of the cell's lateral walls.

The perfect arrangement of the hard spheres described above corresponds to their maximum packing density within the cell. This also relates to the minimum porosity of this model of a porous medium. When it is not possible to arrange all the spheres in the required order, defects form, as illustrated in the lower right corner of the cell in Fig. 1. A large number of such defects can affect the porosity of the cell; therefore, in experiments for measuring the diffusion coefficient, such defects are either absent or are of short length.

The experiments employing spheres with a diameter of d_1 are conducted in the cell of various thicknesses $h = 2.00 \pm 0.01, 2.19 \pm 0.01, 2.48 \pm 0.01$, and 2.70 ± 0.01 mm, thereby providing the option to vary the porosity of the cell (Fig. 2*b*). The distinction between this form of ordered packing and the one illustrated in Fig. 2*a* is that the spheres come into contact with only one wall of the cell.

In the study, we calculate the porosity P of the porous medium as the ratio of the total volume of all pores in the porous medium to the volume of a rectangular cell. The pore volume is measured by means of a syringe pump, which enables the precise calculation of the volume of water pumped. The volume of the cell is calculated using the formula $V = lbh$. The results of the porosity calculations for all porous media models are presented in Table 1.

In the experiments, the lower half of the vertical cell is filled with an aqueous solution of Rhodamine B and sodium chloride, while the upper half of the cell is filled with pure water (Fig. 3). The addition of sodium chloride to the water results in an increase in the density of the Rhodamine B solution, thereby preventing the unwanted mixing of the upper and lower fluids. The quantity of sodium chloride is chosen so that the density of the aqueous solution of Rhodamine B and sodium chloride equals 1.02 g/cm^3. This density is obtained at a sodium chloride concentration of 0.72 mol/L.

An aqueous solution Rhodamine B has fluorescence properties, with a peak emission wavelength of 610 nm (orange light) and a peak excitation wavelength of 550 nm (green light). In our experiments, the cell is illuminated by a 1-W laser (*2* in fig. 1) emitting at a wavelength of 532 nm (green light), with a beam divergence angle of 20°. The illuminated part of the cell is recorded by a Canon EOS 60D photo camera (*3* in

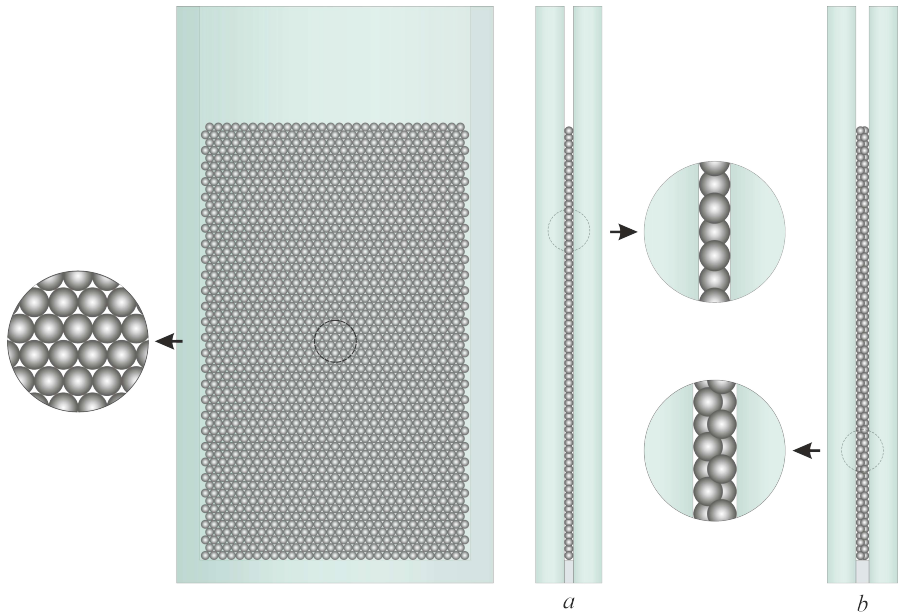


Figure 2 The arrangement of spheres in a rectangular cell: (*a*) a hexagonal arrangement corresponds to M1, M5, and M6; (*b*) a configuration where hard spheres touch opposite cell walls (M2 - M4)

fig. 1) with a Tamron AF 90 mm F/2.8 Macro lens and LPF565 orange filter, having a cutoff wavelength of 656 ± 15 nm. The Powell lens is used to generate a laser sheet of an approximately constant intensity throughout its length.

When the Rhodamine B-containing water comes into contact with pure water, a diffusion zone is formed. Within this zone, the concentration of Rhodamine B decreases from a maximum value in the lower fluid to a minimum value in the upper one. The width of the diffusion zone increases over time due to molecular diffusion of Rhodamine B from the lower fluid into the upper one. The rate of growth of the diffusion zone can be measured, and thus the diffusion coefficient can be calculated.

In order to determine the effect of sodium chloride added to water on the results of measurements of the diffusion coefficient of Rhodamine B in water, a series of experiments was conducted in a previous study of the authors [22]. In those experiments, Rhodamine B and sodium chloride were dissolved in the same fluid and in different fluids. In the first series of experiments, aqueous solutions of Rhodamine B and sodium chloride and pure water were used. In the second series of experiments, the lower half of the cell was filled by an aqueous solution of sodium chloride (a denser fluid), while the upper half of the cell was filled with an aqueous solution of Rhodamine B (a less dense fluid: The concentration of Rhodamine B was very low and did not affect the density of pure water). In both series of experiments, the diffusion coefficient of Rhodamine B in water was measured, and it was found to be unchanged.

It is observed from the experimental findings that the diffusion coefficient D_m measured in experiments with a cell filled exclusively with fluids differs from the diffusion coefficient D_p measured under conditions where the cell is filled with fluids

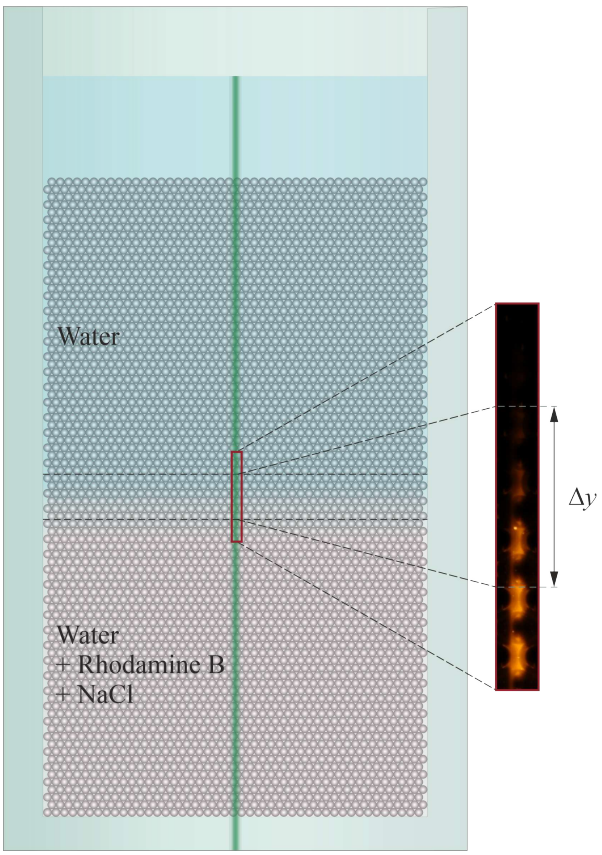


Figure 3 (left) Scheme of a vertical cell filled with hard spheres and an aqueous solution of Rhodamine B and sodium chloride; (right) photo of a section of the cell illuminated by a vertical laser sheet at $t = 4$ hours after the beginning of the experiment with M1. The region between horizontal dashed lines illustrates the diffusion zone, within which the concentration of Rhodamine B varies from a maximum value of $C = 1$ to a minimum value of $C = 0$

and hard spheres. The ratio of these diffusion coefficients is equal to the diffusion tortuosity:

$$\tau_d = \frac{D_m}{D_p}. \tag{1}$$

The objective of the present series of experiments is to determine the tortuosity of the porous media models under consideration. The research is focused on the measurement of the diffusion coefficient of Rhodamine B in water D_p in the cell filled with hard spheres. This is due to the fact that the authors employed the experimental technique outlined to measure the molecular diffusion coefficient D_m in a previous study [22]. The resulting value of $D_m = 4.2 \cdot 10^{-6}$ cm^2/s is in good agreement with previously reported data [23–25].

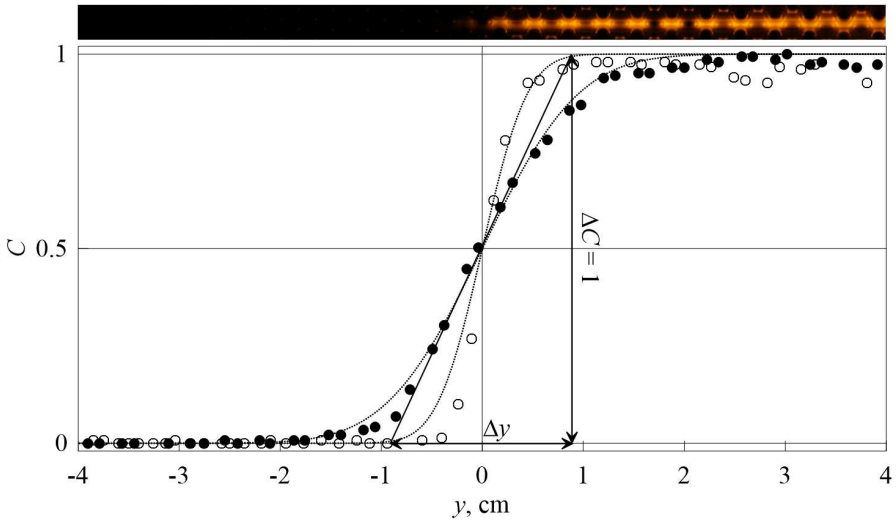


Figure 4 Dependence of the concentration of Rhodamine B in water on the vertical coordinate in an experiment to measure the molecular diffusion coefficient in a porous medium at $t = 0.5$ (empty symbols) and 19 (filled symbols) hours; M2. Data referring to the intensity of the light emission at a time of $t = 0.5$ hours are obtained from the photo presented above the plot

4 Experimental Results

In our experiments, the concentration of the Rhodamine B is determined by laser-induced fluorescence, a technique which is found to be efficient in the study of mass transfer in porous media [22, 26–28]. When illuminated by a green laser beam, an aqueous solution of Rhodamine B emits orange light, which is visible through the camera's orange filter. The photo in Fig. 4 illustrates the variation in the intensity of the emitted orange light along the vertical cell filled with hard spheres. Three distinct regions can be identified. The first region is where the aqueous solution of Rhodamine B emits orange light that is uniform along the vertical axis. The second region is a transition zone near the interface between the two fluids, where the radiation intensity decreases from its maximum value to zero. The third region is a dark region within the upper fluid, where the radiation of Rhodamine B is zero everywhere.

The intensity of the radiation inside the laser sheet is dependent on both the longitudinal and transverse coordinates. In order to eliminate errors associated with variations in radiation intensity across the laser sheet, we measure the radiation intensity in the pores between the hard spheres in the vicinity of the axis of the laser sheet. Figure 5*a* shows a section of a photo of the cell, in which the measurement points for the radiation intensity of an aqueous solution of Rhodamine B are indicated by green symbols. To avoid errors associated with the incorrect determination of the position of the pores between the hard spheres, an overlay of photos is used. More specifically, a photo illustrating the radiation intensity of Rhodamine B in water (Fig. 5*a*) is overlaid on the photo showing the packing of hard spheres (Fig. 5*b*).

The photos obtained in the experiments are then converted to a grayscale, where each pixel corresponds to a color number N in an 8-bit range from 0 to 255. Here,

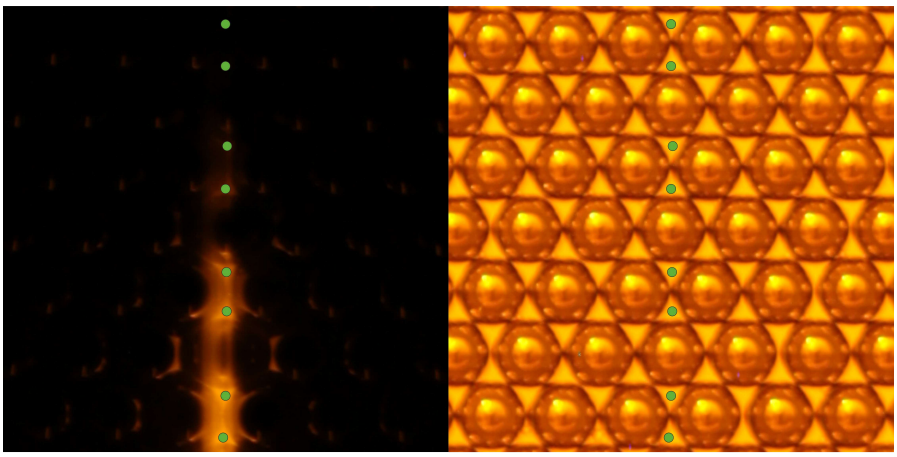


Figure 5 (a) A photograph of a sector of the rectangular cell (M2) illustrating the intensity of the light emitted by an aqueous solution of Rhodamine B within the diffusion zone when illuminated by a laser sheet; (b) A photograph of the same sector under room lighting. The green symbols indicate points where the intensity of the aqueous solution of Rhodamine B is measured. The size of the cell sector is 12×12 mm^2

$N = 0$ corresponds to black pixels, and $N = 255$ to white pixels. When measuring the width of the diffusion zone, it is assumed that the concentration of Rhodamine B is proportional to the brightness of the fluid. Then, one can convert from the color number N to the concentration C by scaling the measured value by the maximum brightness recorded in the region under consideration.

The experimental data points on the plot in Fig. 4 illustrate the change in concentration of Rhodamine B in water from the minimum value $C = 0$ to the maximum value $C = 1$ within the cell at time $t = 0.5$ and 19 hours (empty and filled symbols, respectively). The origin of the coordinate axis $y = 0$ indicates the position of the interface between the aqueous solution of Rhodamine B and pure water at the moment of contact between them. There is a clear correlation between the decrease in solute concentration in an aqueous solution of Rhodamine B (on the right-hand side of the plot) and the increase in the concentration of Rhodamine B in pure water (on the left-hand side of the plot). The dotted lines are a result of calculations for the concentration of the solute $C(y, t)$ in the form of complementary error functions [29]. It is evident that the experimental data align closely with the theoretical predictions when $t = 19$ hours (filled symbols), and there is a slight discrepancy when $t = 0.5$ hours. The possible reasons for this discrepancy will be considered when discussing the data in Fig. 6. It is important to note that the complementary error function alone does not allow us to precisely determine the boundaries of the diffusion zone, because it asymptotically approaches $C = 0$ and $C = 1$. For this reason, we propose determining the boundaries of the diffusion zone by finding the points where the tangent line at $y = 0$ intersects the lines $C = 0$ and $C = 1$.

A comparison of the experimental data obtained at different times (empty and filled symbols in Fig. 4) demonstrates that the width Δy of the diffusion zone increases over

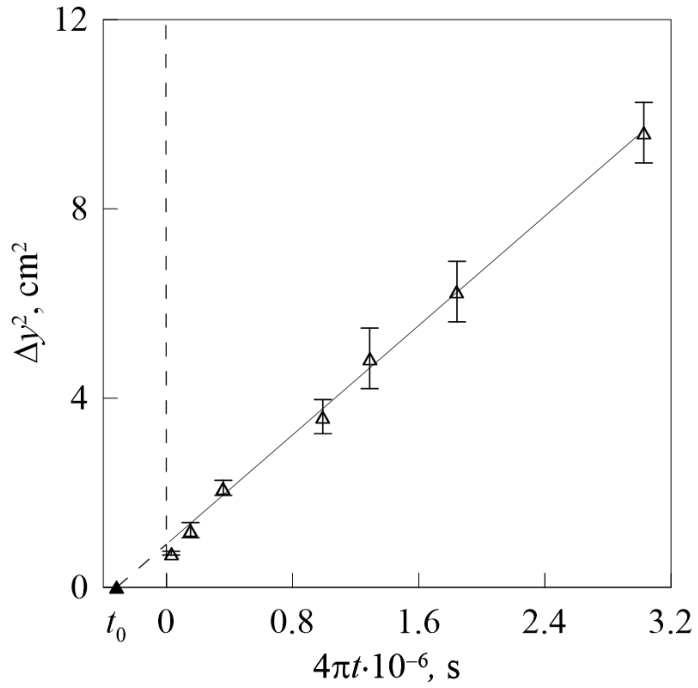


Figure 6 Time evolution of the square of the diffusion zone width in an experiment with M1. The slope of the line is equal to $D_p = 2.89 \cdot 10^{-6}$ cm^2/s. Empty symbols illustrate the experimental data, while the filled symbol indicates the extrapolated value of time corresponding to the zero width of the diffusion zone

time. Theoretical predictions [29] and experimental measurements [22, 28, 30] demonstrate that the square of the width of the diffusion zone varies over time according to the law

$$D = \frac{\Delta y^2}{4\pi t}. \tag{2}$$

Figure 6 demonstrates the results of measurements of the squared width of the diffusion zone as a function of the parameter $4\pi t$ in a 2-mm-thick cell. Here, time t is measured from the moment the contact line originates between the aqueous solution of Rhodamine B and pure water. As the cell is slowly filled with water, it takes several tens of minutes from the formation of the initial diffusion zone until the cell is completely filled with fluids and recording starts. For this reason, the first experimental data point is obtained at a time $t > 0$. Furthermore, during the initial phase of the experiment, a transient process lasting approximately three hours is detected. This is then followed by the start of the main phase of the experiment, which lasts several dozen hours. The presence of a transition process is explained by the formation of a narrow (several millimetres wide) mixing zone at the interface between two fluids during the filling process. Within this zone, the concentration distribution of Rhodamine B differs from the distribution that arises due to diffusion. The time required for the formation of a solute concentration gradient corresponding to the diffusion process

is a key factor in determining the duration of the initial phase of the experiment. Therefore, this time is not taken into account in the measurements; data processing is performed only for the main phase of the experiment.

The results of measurements of the squared width of the diffusion zone as a function of time in the main phase of the experiment show that it varies according to the law $\Delta y^2 = 2.89 \cdot 10^{-6} 4\pi t$ cm^2. It follows from Eq. 2 that the diffusion coefficient D_p of Rhodamine B in water in the porous medium used is equal to $2.89 \cdot 10^{-6}$ cm^2/s.

In experiments, the initial thickness of the unwanted mixing zone may vary. In order to ensure a correct comparison of experimental results, it is necessary to determine the time t_0 corresponding to a zero thickness of the diffusion zone. To do this, the solid line in Fig. 6 is extrapolated to the value $\Delta y = 0$. A shift in the zero time value does not have a notable effect on the measured value of diffusion coefficient D_p since the typical duration of the main phase of the experiment is significantly greater than the observed time shift t_0.

Figure 7 indicates the results of measurements of the square of the diffusion zone width Δy^2 as a function of time $4\pi t$ for porous media formed by hard spheres with a diameter $d = 1.98$ mm. The porous media are formed by hard spheres with a diameter d and various cell thicknesses h. The data in Fig. 7 are presented with the time origin shifted by t_0. For all values of h, the experimental data are well approximated by straight lines. Therefore, the square of the diffusion zone width increases linearly with time. Furthermore, the slope for each line is equal to the diffusion coefficient D_p. The diffusion coefficient D_p increases with an increase in the cell thickness h. This is due to a change in the geometry of the pore space caused by changes in the distance between the wide cell walls.

Experiments conducted with hard spheres of diameters $d = 1.98$, 3.00, and 3.98 mm in (M1, M5, and M6 in Table 1) show that the slope of the function $\Delta y^2(4\pi t)$ is universal for all data (Fig. 8). Therefore, the diffusion coefficient D_p is independent on the size of the spheres for all porous media of this type.

A comparison of the coefficients D_p obtained from Fig. 7 and Fig. 8 with the molecular diffusion coefficient D_m indicates that the transport of the fluorescent dye in water filling the porous medium occurs at a slower rate than in free water. This finding is consistent with the concept that the trajectories of solute molecules in porous materials are tortuous since the molecules are obliged to avoid the rigid components of the porous medium. The obtained data on the diffusion coefficients D_p can be used to calculate the tortuosity of the porous medium. Substitution of the values of D_p into Eq. 1 yields the tortuosity values τ (Table 1).

5 Discussion

As outlined in the Introduction, there are several types of tortuosity, including geometric, hydraulic, diffusion and electrical. In our work, we determine the diffusion coefficients of Rhodamine B in free water and in water saturating a porous medium, and can therefore determine the diffusion tortuosity $\tau_d = \frac{D_m}{D_p}$. To the best of our knowledge, there are very few experimental studies in which τ_d has been determined for porous materials whose skeleton resembles a fixed bed of hard spheres.

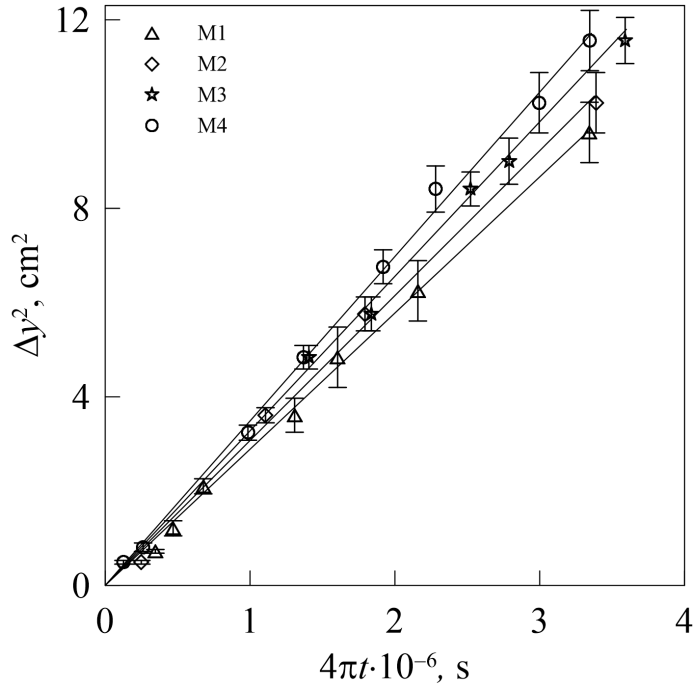


Figure 7 Time evolution of the square of the diffusion zone width in experiments with M1 – M4

Currie [31, 32] measured the diffusion coefficient of hydrogen in free air and inside a cylindrical column filled by granular materials. The author used a thermal conductivity detector for this purpose. Currie's research focused on the diffusion of hydrogen in air across a range of granular materials, including monosized glass beads and glass bead mixtures. Through the controlled variation of the composition of the beads it was possible to alter the porosity of the material. This, in turn, resulted in an alteration in its tortuosity. The measurement results obtained in experiments with porous media, consisting of monosized beads or beads of different diameters, are plotted in the plane (P, τ_d) (triangles in Fig. 9).

Delgado [33] used a rather simple experimental technique to measure the diffusion coefficient of NaCl in water. The porous medium was constituted of a cylindrical column filled with silica particles and pure water. The silica particles varied in diameter, enabling the porosity and tortuosity of the porous medium to be modified by adjusting the mixture of particles. Above the column, a layer of saline water was located, the concentration of NaCl within which decreased due to diffusion through the porous medium. By measuring the electrical conductivity of the saline water, the author was able to determine the change in NaCl concentration and, consequently, the diffusion coefficient. The measurement results are illustrated as circles in Fig. 9.

The findings derived from the analysis of new experimental data are illustrated in Fig. 9 as squares and a diamond. A comparison of the previous results with those obtained in this study indicates that the new data are obtained under conditions of relatively high porosity $P > 0.4$, while others worked in the range of moderate

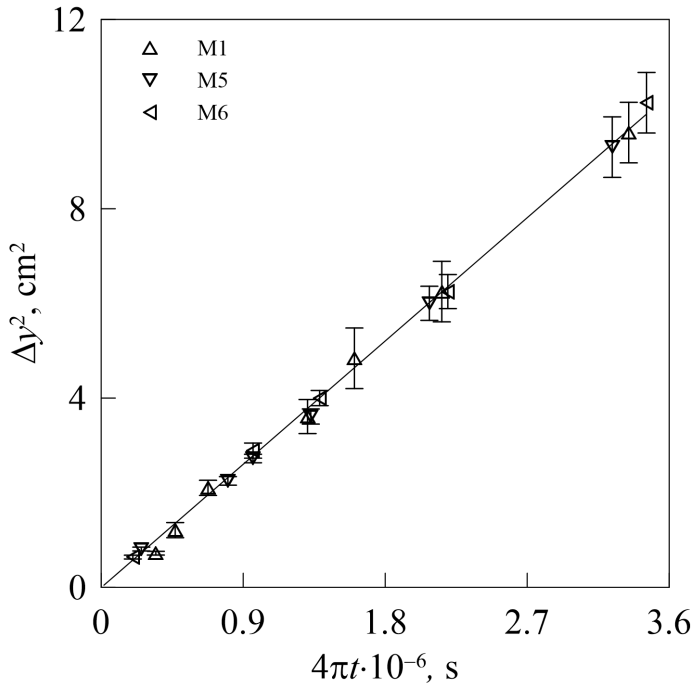


Figure 8 Time evolution of the square of the diffusion zone width in experiments with M1, M5, and M6. The slope of the solid line is equal to $D_p = 2.89 \cdot 10^{-6}$ cm^2/s

porosities $0.2 < P < 0.4$. The two measurement ranges overlap only at the point $P \approx 0.4$, a scenario in which the particle diameter is equal to the gap thickness in our experiments (diamond in Fig. 9). Here, symbol $\diamond$ illustrates the average value of tortuosity obtained in experiments with M1, M5, and M6.

At first sight, the previously obtained data and the new experimental results appear to be in good agreement with one another and can be described by the universal relation $t_d = 2.15 - 1.75P$ (not shown in Fig. 9). However, this type of relation $\tau_d - P$ is not typical for porous materials. Figure 9 further illustrates the results of theoretical calculations of the tortuosity of a bed of spherical particles. Weissberg [9] analyzed the effective diffusion of solute in a fluid which fills the void regions of the fixed bed of spheres. The calculations were simplified by considering an idealized bed in which centers are randomly situated without restricting the spheres to nonoverlapping locations. The result, applicable to randomly overlapping spheres of either uniform or nonuniform sizes, gives the diffusion tortuosity as

$$\tau_d = 1 - 0.5 \ln P. \tag{3}$$

The results of the calculations using Eq. 3 are shown in Fig. 9 as a dotted line. As illustrated, the theoretical calculations agree well with previously published data (filled symbols) and with the results on tortuosity calculations from our experiments with densely packed hard spheres (M1, M5, and M6).

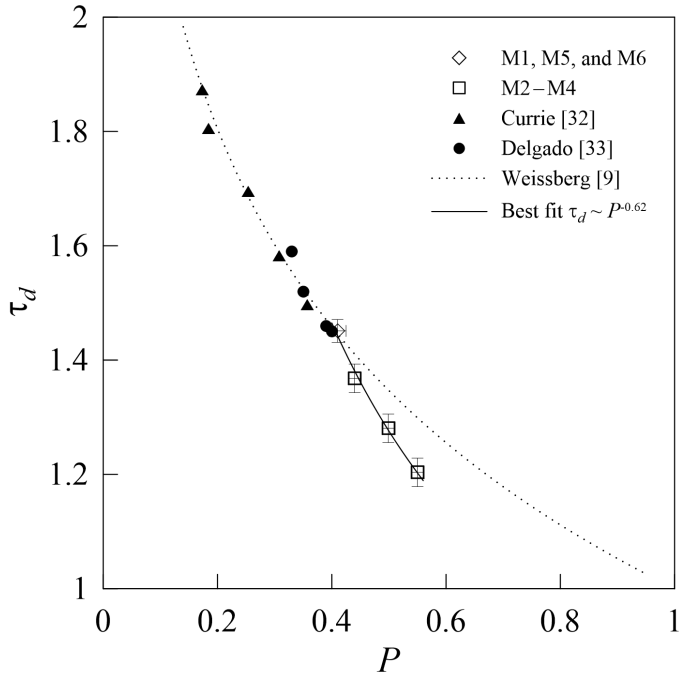


Figure 9 Dependence of the tortuosity of a porous medium on its porosity. The dotted line illustrates the results of theoretical calculations of diffusion tortuosity [9]. The squares indicate the results from experiments with M2 - M4, while the diamond denotes the average tortuosity obtained from experiments with M1, M5, and M6. The circles and triangles represent the results of experiments measuring the diffusion tortuosity of a porous medium composed of silica particles [33] and mixtures of hard spheres of varying diameters [32], respectively

Let us discuss the potential reasons for the discrepancy between the new experimental data and the values predicted by Eq. 3. The discrepancy between theory and experiment is only evident in the M2 – M4 experiments, where the packing of hard spheres is not dense and the spheres in neighbouring rows contact opposite walls of the cell (Fig. 2b). One potential explanation for this phenomenon is that the local porosity (consequently, the tortuosity) of the packing in the region where the diffusion coefficient is measured differs from the total porosity of the entire porous medium. However, this hypothesis is contradicted by the fact that the hard spheres were packed in a regular manner (the technique for manufacturing porous media is discussed in detail in Section 3). The local porosity displays periodic variations along the vertical axis since upward-moving solute molecules meet hard spheres resting against one wall and then the other. The cross-section available for solute diffusion therefore changes. The maximum width of the diffusion zone in the experiments is approximately equal to 3 cm, whilst the size of the pores varies with a spatial period of the order of the diameter of the spheres. Consequently, the values of D_p and τ_d obtained in the experiments are the result of averaging a large number of pores, rather than being a function of local porosity. The decision to compare our results with data from experimental studies [32, 33] and with the theoretical predictions [9] is based on the assumption that the

diffusion tortuosity of materials depends not only on porosity but also on pore shape. The latter suggests that, in terms of their effect on solute diffusion, the pores between hard spheres in wide channels are similar to the pores between spheres and between spheres and the walls in narrow channels. Probably, this is most relevant for densely packed spheres, where $P < 0.4$.

Finally, we determine the relation $\tau_d - P$ that describes new experimental results. To do this, we use a widely accepted empirical tortuosity–porosity relation $\tau = AP^{m-1}$ with adjustable parameters A and m (for example, [3]). Here, parameter A and the exponent m are dependent on the type of tortuosity and the shape of the skeleton. The best fit is $\tau_d = 0.83P^{-0.62}$ with $A = 0.83$ and $m = 1.62$ (solid line in Fig. 9). When considering a porous medium composed of spherical particles, m ranges from 1.3 to 1.8 [13]. This approach to describing tortuosity indicates that new experimental data are consistent with the results of other authors.

6 Conclusion

The paper presents the findings from calculations of diffusion tortuosity τ_d, obtained using an experimental technique that enables the measurement of the molecular diffusion coefficient D_m and the diffusion coefficient D_p of a solute in a fluid saturating the pores of a porous medium. By calculating the ratio of these coefficients, the diffusion tortuosity of the porous medium is determined. The dependence of tortuosity on porosity P is studied, with porosity varied by changing the distance between the walls of a rectangular cell filled with monosized hard spheres. The new experimental results are then compared with theoretical predictions and empirical data on diffusion tortuosity obtained for porous media whose skeleton is formed by spherical particles. The new results align closely with those previously obtained by other researchers in the limiting case of densely packed spheres but differ from theoretical predictions for loose porous media.

7 Funding

The work is supported by the Ministry of Education of the Russian Federation (Registration number:1025032600036-8-2.3.2).

References

[1] Ghanbarian, B., Hunt, A.G., Ewing, R.P., Sahimi, M.: Tortuosity in porous media: a critical review. Soil science society of America journal **77**(5), 1461–1477 (2013)

[2] Clennell, M.B.: Tortuosity: a guide through the maze. Geological Society, London, Special Publications **122**(1), 299–344 (1997)

[3] Shen, L., Chen, Z.: Critical review of the impact of tortuosity on diffusion. Chemical Engineering Science **62**(14), 3748–3755 (2007)

[4] Holzer, L., Marmet, P., Fingerle, M., Wiegmann, A., Neumann, M., Schmidt, V.: Tortuosity and Microstructure Effects in Porous Media: Classical Theories, Empirical Data and Modern Methods, p. 190. Springer, Cham (2023)

[5] Koponen, A., Kataja, M., Timonen, J.: Tortuous flow in porous media. Phys. Rev. E. **54**, 406–410 (1996)

[6] Dias, R., Teixeira, J.A., Mota, M., Yelshin, A.: Tortuosity variation in a low density binary particulate bed. Separation and Purification Technology **51**(2), 180–184 (2006)

[7] Coleman, S., Vassilicos, J.: Transport properties of saturated and unsaturated porous fractal materials. Physical Review Letters **100**(3), 035504 (2008)

[8] Pisani, L.: Simple expression for the tortuosity of porous media. Transport in Porous Media **88**, 193–203 (2011)

[9] Weissberg, H.L.: Effective diffusion coefficient in porous media. Journal of Applied Physics **34**(9), 2636–2639 (1963)

[10] Silva, M.T.Q.S., Rocio Cardoso, M., Veronese, C.M.P., Mazer, W.: Tortuosity: A brief review. Materials Today: Proceedings **58**, 1344–1349 (2022)

[11] Iversen, N., Jørgensen, B.B.: Diffusion coefficients of sulfate and methane in marine sediments: Influence of porosity. Geochimica et Cosmochimica Acta **57**(3), 571–578 (1993)

[12] Moldrup, P., Olesen, T., Komatsu, T., Schjønning, P., Rolston, D.: Tortuosity, diffusivity, and permeability in the soil liquid and gaseous phases. Soil Science Society of America Journal **65**(3), 613–623 (2001)

[13] Friedman, S.P.: Soil properties influencing apparent electrical conductivity: a review. Computers and electronics in agriculture **46**(1-3), 45–70 (2005)

[14] Fu, J., Thomas, H.R., Li, C.: Tortuosity of porous media: Image analysis and physical simulation. Earth-Science Reviews **212**, 103439 (2021)

[15] Yun, M., Yu, B., Xu, P., Wu, J.: Geometrical models for tortuosity of streamlines in three-dimensional porous media. The Canadian Journal of Chemical Engineering **84**(3), 301–309 (2006)

[16] Rao, D., Bai, B.: Study of the factors influencing diffusive tortuosity based on pore-scale sph simulation of granular soil. Transport in Porous Media **132**, 333–353 (2020)

[17] Comiti, J., Renaud, M.: A new model for determining mean structure parameters of fixed beds from pressure drop measurements: Application to beds packed with parallelepipedal particles. Chemical Engineering Science **44**(7), 1539–1545 (1989)

[18] Tsai, D.-S., Strieder, W.: Effective conductivities of random fiber beds. Chemical Engineering Communications **40**(1–6), 207–218 (1986)

[19] Yun, M.-J., Yue, Y., Yu, B.-M., Lu, J.-D., Zheng, W.: A geometrical model for tortuosity of tortuous streamlines in porous media with cylindrical particles. Chinese Physics Letters **27**(10), 104704 (2010)

[20] Wyllie, M.R.J., Gregory, A.R.: Fluid flow through unconsolidated porous aggregates: Effect of porosity and particle shape on kozeny–carman constants. Industrial & Engineering Chemistry **47**(7), 1379–1388 (1955)

[21] Rodrigues, S.J., Vorhauer-Huget, N., Richter, T., Tsotsas, E.: Influence of particle shape on tortuosity of non-spherical particle packed beds. Processes **11**(1), 3 (2022)

[22] Bushueva, A., Polezhaev, D.: Mass transfer of solute in an oscillating flow in a two-dimensional channel. Physics of Fluids **36**(4) (2024)

[23] Culbertson, C.T., Jacobson, S.C., Ramsey, J.M.: Diffusion coefficient measurements in microfluidic devices. Talanta **56**(2), 365–373 (2002)

[24] Gendron, P.-O., Avaltroni, F., Wilkinson, K.: Diffusion coefficients of several rhodamine derivatives as determined by pulsed field gradient–nuclear magnetic resonance and fluorescence correlation spectroscopy. Journal of fluorescence **18**(6), 1093–1101 (2008)

[25] Fang, X., Xuan, Y., Li, Q.: Experimental investigation on enhanced mass transfer in nanofluids. Applied Physics Letters **95**(20) (2009)

[26] Roth, E.J., Mays, D.C., Neupauer, R.M., Sather, L.J., Crimaldi, J.P.: Methods for laser-induced fluorescence imaging of solute plumes at the darcy scale in quasi-two-dimensional, refractive index-matched porous media. Transport in Porous Media **136**, 879–898 (2021)

[27] Kong, X.-Z., Ahkami, M., Naets, I., Saar, M.O.: The role of high-permeability inclusion on solute transport in a 3d-printed fractured porous medium: An lif–piv integrated study. Transport in Porous Media **146**, 283–305 (2023)

[28] Polezhaev, D., Teryokhina, A.: Solute transport in a porous medium in the presence of oscillations. Journal of Applied Mechanics and Technical Physics **66**(6), 1090–1104 (2025)

[29] Crank, J.: The Mathematics of Diffusion, 2nd edn., p. 347. Oxford University Press, Oxford (1975)

[30] Rashidnia, N., Balasubramaniam, R., Kuang, J., Petitjeans, P., Maxworthy, T.:

Measurement of the diffusion coefficient of miscible fluids using both interferometry and wiener's method. International Journal of Thermophysics **22**(2), 547–555 (2001)

[31] Currie, J.A.: Gaseous diffusion in porous media. part 1—a non-steady state method. British Journal of Applied Physics **11**(8), 314–317 (1960)

[32] Currie, J.: Gaseous diffusion in porous media. part 2.-dry granular materials. British Journal of Applied Physics **11**(8), 318–324 (1960)

[33] Delgado, J.M.P.Q.: A simple experimental technique to measure tortuosity in packed beds. The Canadian Journal of Chemical Engineering **84**(6), 651–655 (2006)